Title:

Oligodendrocyte heterogeneity in the mouse juvenile and adult central nervous system

Authors:

Sueli Marques[1†], Amit Zeisel[1†], Simone Codeluppi[1], David van Bruggen[1], Ana Mendanha Falcão[1], Lin Xiao[3], Huiliang Li[3], Martin Häring[1], Hannah Hochgerner[1], Roman A. Romanov[1,2], Daniel Gyllborg[1], Ana Muñoz Manchado[1], Gioele La Manno[1], Peter Lönnerberg[1], Elisa M. Floriddia[1], Fatemah Rezayee[1], Patrik Ernfors[1], Ernest Arenas[1], Jens Hjerling-Leffler[1], Tibor Harkany[1,2], William D. Richardson[3], Sten Linnarsson[1*], Gonçalo Castelo-Branco[1*]

Affiliations:

[1] Laboratory of Molecular Neurobiology, Department Medical Biochemistry and Biophysics, Karolinska Institutet, Stockholm, Sweden

[2] Department of Molecular Neurosciences, Center for Brain Research, Medical University of Vienna, Austria

[3] Wolfson Institute for Biomedical Research, University College London, Gower Street, London WC1E 6BT, United Kingdom

[†] equal contribution

*Correspondence to: sten.linnarsson@ki.se, goncalo.castelo-branco@ki.se

Abstract:

Oligodendrocytes have been broadly considered as a functionally homogenous population in the central nervous system (CNS). We performed single-cell RNA-Seq on 5072 cells of the oligodendrocyte lineage from ten regions of the mouse juvenile/adult CNS. Twelve populations were identified, representing a continuum from *Pdgfra*+ oligodendrocyte precursors (OPCs) to distinct mature oligodendrocytes. Initial stages of differentiation were similar across the juvenile CNS, whereas subsets of mature oligodendrocytes were enriched in specific regions in the adult brain. Newly-formed oligodendrocytes were found to be resident in the adult CNS and responsive to complex motor learning. A second *Pdgfra*+ population, distinct from OPCs, was found along vessels. Our study reveals the dynamics of oligodendrocyte differentiation and maturation, uncoupling them at a transcriptional level and highlighting oligodendrocyte heterogeneity in the CNS.

One Sentence Summary:
Transcriptional heterogeneity of oligodendrocytes across the juvenile and adult mouse central nervous system

Main Text:

Oligodendrocytes ensheath axons in the CNS, allowing rapid saltatory conduction and providing metabolic support to neurons. A largely homogeneous population is thought to execute these functions throughout the CNS (*1*). Nevertheless, Del Rio Hortega originally described oligodendrocytes as a morphologically heterogeneous cell population (*2*) and subsequent studies have reinforced this view. It is thus unclear whether oligodendrocytes constitute a homogeneous cell population that becomes morphologically diversified during maturation through interactions within the local environment, or whether there is intrinsic functional heterogeneity (*3-5*).

We analyzed 5072 transcriptomes of single cells expressing markers from the oligodendrocyte lineage, isolated from ten distinct regions of the anterior-posterior and dorsal-ventral axis of the mouse juvenile and adult CNS (Fig. 1A, 1B, S1A and 4). Biclustering analysis by BackSpinV2 (*6*) led to the identification of thirteen distinct cell populations (Fig. 1C, S1B and S14). Analysis of clustering results by heatmap (Fig. S1B), pairwise correlation (Fig. 1C) and t-Distributed Stochastic Neighbor Embedding (t-SNE) projection (Fig. 2A) indicated a transcriptional continuum encompassing stages in the differentiation program from OPCs to mature oligodendrocytes. Hierarchical clustering (Fig. 1C) and differential expression analysis (Tables S1 and S2) lead to the assignment of the identified populations in the following categories: *Pdgfra+* vascular and leptomeningeal cells (VLMCs), segregated from other oligodendrocyte lineage cells; *Pdgfra+* OPCs; differentiation-committed oligodendrocyte precursors (COPs); newly-formed oligodendrocytes (NFOL1-2); myelin-forming oligodendrocytes (MFOL1-2); mature oligodendrocytes (MOL1-6). The t-SNE projection indicated a narrow differentiation path connecting OPCs and myelin-forming oligodendrocytes, diversifying into 6 mature states (Fig. 2A).

OPCs expressed canonical markers (*Pdgfra* and *Cspg4*), previously identified markers (*Ptprz1* and *Pcdh15 (7)*) and novel markers such as *Kcnip3, Emid1* and *Tmem100* (Figs. 2B, S1B and S9). 10% of OPCs co-expressed cell cycle genes (Figs. 2C and S2D), consistent with the reported average cell cycle time of 19 days in the cortex at post-natal day (P) 21 (*8*). Several of the novel markers identified in OPCs were previously associated with astrocytes/radial glia (*6*), such as *Fabp7*, *Emid1* and *Tmem100* (Figs. S1B, S3 and S9), consistent with the origin of OPCs from radial glia-like cells in the ventricular zone. OPCs have been shown to be able to generate some astrocytes during development but lose such capacity in adult CNS, although they can re-acquire this ability in certain injury paradigms (*9*).

Differentiation-committed oligodendrocyte precursors (COP) presented several markers of OPCs, including *Sox6* (Fig. 2B), essential to keep oligodendrocytes undifferentiated and migratory prior to myelination (*10*), and uniquely expressed *Bmp4* (Fig. 2B), an inhibitor of oligodendrocyte differentiation (*11*). These cells expressed higher levels of *Gpr17*, another inhibitor of oligodendrocyte differentiation (*12*), *Neu4* and *Vcan* (Figs. 2B, 2D, S1B, S4 and S9). Committed oligodendrocyte precursors were distinct from OPCs, since they did not express *Pdgfra* and *Cspg4* (Fig. 2B) and presented a lower average of expression of cell cycle markers (Fig. 2C and S2D). Several genes involved in migration (*Tns3* and *Fyn*) were expressed in this population (Fig. S9).

Newly-formed oligodendrocytes (NFOL) 1 and 2 expressed genes induced at early stages of differentiation (*13-15*) (*Tcf7l2*, *Mpzl1* and *Casr*, Fig. S9). *Gpr17* was decreased compared to committed oligodendrocyte precursors (Fig. 2B), while the expression of *Tcf7l2*, involved in

oligodendrocyte differentiation (*16*), peaked in this group of cells (Fig. S9). Newly-formed oligodendrocytes are most likely migratory, expressing *Tns3, Plxnb3* and *Rasgef1b*. NFOL2 presented higher levels of *Sema6a* (positive regulator of oligodendrocyte cytoskeleton dynamics, process extension and maturation) and started expressing in higher levels genes involved in adhesion (*Sh3gl3 and Ninj1)*.

Myelin-forming oligodendrocytes had higher expression of *Mal* and *Mog* (Fig. S1A), *Cldn11* and *Plp1* (required for the maintenance of compact myelin sheaths) *(17)* and adhesion genes (*Cdh19* and *Igsf8*). Genes responsible for myelin formation (*Tmem10/Opalin*, *Serinc5*) were first present in these populations (Fig. S1B). Single-molecule fluorescence RNA in situ hybridization (smFISH) indicated that myelin forming populations (*Ctps+*) were distinct from mature oligodendrocytes (*Klk6+*, Fig. 2E and S4). Mature populations (MOL1-6) expressed late oligodendrocyte differentiation genes (*13*) such as *Klk6*, *Apod* and genes present in myelinating cells (transferrin (*Trf*) and *Pmp22*) (Fig. S1B).

In order to identify sequential genes expression, each cell was projected on a pseudo-time along the transition from OPC to myelin-forming cell (on the tSNE plan) (Fig. 2F). Applying the unsupervised algorithm Monocle (*18*) confirmed the ordering of cell types (Fig. S2A). We could also identify several known transcription factors involved in oligodendrocytes development, including *Sox6, Nkx2.2 and Nkx2.9,* but also novel such as *Etv6*, *Onecut2*, *Sox21, Etv1 and Hopx* (Fig. 2F and S9), whose function is likely to be important for transitions between the identified cell states.

We identified a second *Pdgfra+* population, vascular and leptomeningeal cells (VLMC), distinct from OPCs (Fig. 1C and 2A). This population was also found when sorting GFP+ cells from *Pdgfra*-H2B-GFP (*19*) and *Pdgfra*-Cre-RCE (LoxP-GFP) mice (*20*) (Fig. S2B). These cells exhibited low levels of *Cspg4* (NG2) (Fig. 2B), specifically expressed *Lum* (Fig. 2B and S4), presented markers of the pericyte lineage (*Vtn, Col1a1* and *Col1a2*, Fig. 2B, S1B and S2C) and produced laminins (*Lama1*, *Lama2*) and collagens (*Col4a5*, *Col4a6*) characteristic of the basal lamina. Their unique identity was confirmed using smFISH and immunohistochemistry, which also indicated that *Pdgfra+/Sox10-* VLMCs were localized on blood vessels (Fig. 2G and S4) and the meninges (Fig. S10A, B). In contrast, *Col1a1-/Pdgfra+* OPCs were distributed in the parenchyma, in close association but not overlapping with the vasculature (Fig. 2G), as recently reported (*21*). Clustering analysis indicated that this population is indeed related but nevertheless distinct from pericytes, which have been reported to be NG2+ (*22*). VLMCs specifically exhibited markers present in transcriptomes of OPCs isolated in methodologies based on *Pdgfra+* immunoreactivity (Fig. 2B, S1B and S3)(*15*), most likely previously assigned to OPCs due to co-purification of these two populations of cells. As such, VLMCs constitute a distinct *Pdgfra+* population related to pericytes.

We retrieved the fifty genes that better differentiate every branch of the dendrogram plot in Fig. 1C and investigated their putative functional category by gene ontology (GO) (Fig. S5-8, Tables S1-S2). VLMCs were enriched in genes involved in blood vessel development/morphogenesis, and response to wounding (Fig. S5), consistent with their assignment to the pericyte lineage. Both OPCs and VLMCs lacked genes involved in ensheathment of neurons and lipid biosynthesis (Fig. S5 and Tables S1, S2). Combined with the clear segregation of OPCs observed in t-SNE (Fig. 2A), GO analysis confirmed that OPCs undergo significant transcriptional changes during commitment to differentiation (Fig. 2F).

We found at least three distinct oligodendrocyte populations corresponding to early stages of differentiation (Fig 2A). Differentiation-committed oligodendrocyte precursors were enriched in cell fate commitment and in adhesion genes, while newly-formed oligodendrocytes already presented genes involved in steroid biosynthesis, ensheathment of neurons and cell projection organization (Fig. S6). These populations exhibited unique expression of *Tcf7l2, Itpr2, Tmem2* and *Pdgfa* (Fig. 3A and S4). *Tcf7l2*, a marker for early differentiation (*23*), was expressed in non-oligodendrocyte lineage cells in specific regions of the CNS (Fig. S10C). In contrast, *Itpr2*, Inositol 1,4,5-Trisphosphate Receptor, Type 2, encoding for a large tetrameric intracellular Ca2+ channel, was more specific to oligodendrocytes and exhibited close to 100% overlap with *Sox10* positive cells (Fig. S10D). We observed that *Itpr2* immunoreactive cells are distinct from *Pdgfra*+ OPCs (Fig. 3B), and lineage tracing using *Pdgfra*-H2B-GFP and *Pdgfra*-Cre-RCE mice confirmed that Itpr2+ cells are indeed progeny of OPCs (Fig. 3C and Fig. S2B). 22±2% and 25±1.5% of the OPC-derived *Pdgfra*-H2B-GFP+ cells were Itpr2+ in the S1 cortex and CA1 hippocampus at P21 respectively, while 43±3.7% double positive cells were found in the corpus callosum (Fig. 3C). This differential distribution of Itpr2+ oligodendrocytes correlates with active and prolonged differentiation in the juvenile rat corpus callosum (*24*), and suggested earlier maturation in cortex and hippocampus. Indeed, we observed that 77±4% and 48±7% of Sox10+ oligodendrocytes were Itpr2+ at P7 in the CA1 hippocampus and somatosensory cortex, respectively (Fig. 3D,E). The percentage of Itpr2+ cells in the corpus callosum at these 2 stages remains fairly constant (47±4% at P7 and 37±1% at P21, Fig. 3E), consistent with the active myelination of this area in rodents until adulthood (*24*). These tissues still presented 10-20% Itpr2+ cells at adult stages (P90, Fig. 3D,E).

To investigate the potential function of the Itpr2+ population in the adult brain, we analysed their dynamics in the corpus callosum of mice engaged in motor learning in the complex wheel paradigm, a process that requires active myelination (*25*). In this paradigm, running on the wheel leads to an increase in the number of proliferating OPCs after 4 days, followed by an increase in oligodendrocytes after 8 days (*25*). However, increased motor skills were already apparent after 2 days in wild type mice, but not in mutant mice that were unable to synthesize new myelin (*25*), suggesting that oligodendrocyte lineage cells contribute to learning already within the first 2 days. We found that the number of Itpr2+/Sox10+ was increased ~50% in mice that ran on the complex wheel for 2 days, relative to non-runners (Fig. 3F,G). Thus, novel motor activity might trigger rapid differentiation of OPCs into Itpr2+ committed precursors/newly-formed oligodendrocytes that contribute to early learning by facilitating electrical transmission, either through the initiation of myelination or some other pre-myelinating function.

In order to perform a region-specific analysis of the dynamics of oligodendrocyte maturation, we determined the composition in terms of the thirteen identified populations of each region (Fig. 1C, Fig. 4A and Fig. S11). Although OPCs in different regions of the CNS have been described to have different morphologies (*26*), we were unable to identify region-specific subpopulations of OPCs in our dataset (Fig. 2A and 4A). Moreover, OPCs from adult (P60) S1 cortex and corpus callosum did not present a different transcriptional profile from juvenile OPCs (Fig. 4B), even if 16% of the juvenile OPCs were in the cell cycle (as determined by the simultaneous expression of more than 2 cell cycle markers, Fig. 2C), compared to ~3% of the adult OPCs. Differentiation-committed oligodendrocyte precursors, newly-formed and myelin forming oligodendrocytes were present in all regions in juvenile mice (Fig. 1C and 4A), supportive of a common path of differentiation between the different regions (Fig. 2A). These populations could also be observed in the adult corpus callosum and somatosensory cortex, albeit in considerably

lower numbers when compared to juvenile mice (Fig. 4B). Based on the distribution of cell types in the juvenile mice, we classified regions as late- (anterior regions such as amygdala and hippocampus), intermediate- (corpus callosum, zona incerta, striatum and hypothalamus) and early-maturing (cortex and posterior regions such as dorsal horn and SN-VTA) (Fig. 4A and S11). These regional differences could result from different timing of oligodendrocyte maturation during post-natal development (*27, 28*). Indeed, myelination first starts in the rat in posterior regions around P7, with mature oligodendrocyte in the rat dorsal horn at the juvenile stage (P21) (*29*). In contrast, myelination in anterior regions of the rodent CNS such as amygdala, hippocampus, striatum and cortex occurs between P21 and P28 (*29*).

Different regions of the CNS were populated by diverse mature oligodendrocytes (Fig.1C and Fig. S11). While some mature oligodendrocyte populations, such as MOL5, were present throughout the regions, we found that the CA1 hippocampus had an enrichment in MOL1, zona incerta in MOL3, hypothalamus in MOL1/5, SN-VTA in MOL2/3, striatum, somatosensory cortex and dorsal horn in MOL5 and corpus callosum in MOL1, 4, 5 and 6 (Fig. S11). Subsets of MOL5 and MOL6, whose mean diameter was lower than newly-formed, myelin-forming and other mature oligodendrocytes (Fig. S12C), were mainly present in somatosensory cortex and corpus callosum in the adult mice (Fig. 4B). Some of these mature oligodendrocyte populations might be intermediate stages or have specific functions in juvenile mice but then disappear in adulthood. In addition, since MOL5 was already present in several regions of the juvenile CNS (Fig. 1C and Fig. S11), final maturation states of oligodendrocyte might already be achieved in the juvenile mice in certain regions of the CNS, such as the dorsal horn, but only in adulthood in others, such as the corpus callosum.

The region-specific distribution of mature oligodendrocyte populations could indicate functional heterogeneity. GO analysis indicated a divergence at the stage of myelin formation, since MFOL1 was enriched in genes involved in ensheathment of neurons and lipid biosynthetic process, while MFOL2 in genes involved in synapse (Fig. S7 and Tables S1/S2). Although mature oligodendrocyte populations share the expression of many genes, some were differentially enriched within populations. In fact, GO analysis (Fig S9, Tables S1/S2) indicated a segregation with MOL1-4 enriched in lipid biosynthesis and myelination genes such as *Far1* and *Pmp22*, and MOL5-6 (adult) enriched for synapse parts such as *Grm3* (metabotropic glutamate receptor, mainly enriched in MOL6)*, Synpr and Jph4.* We confirmed the presence of Grm3 in the oligodendrocyte lineage (*Pdgfra*-Cre-RCE) and specifically in CC1+ mature oligodendrocytes in the juvenile cortex (Fig. S10E). Even within MOL1-4, enriched in myelin-related genes, specific populations, such as MOL3, are more likely to be involved in synaptic activity (Fig. S8 and tables S1/S2). Thus, our data indicate that several mature oligodendrocyte populations express genes associated with synapses and thus might communicate with neurons through structural specialization.

Optic nerve oligodendrocytes can form axon-myelinic synapses, responding to axonal action potentials via glutamate ionotropic NMDA receptors (*30*). Since we found Grm3 in MOLs (Fig. S9 and S10), we analysed the expression of ionotropic and metabotropic glutamate receptors and other ions channels, including TRP (*31*) and potassium channels, in the identified OL populations (Fig. S13). We found that although most glutamate receptor subunits are expressed throughout oligodendrocyte lineage cells, there is preferential expression in some cell populations., with single cells displaying combinations of subunits that might determine function (Fig. S13). Potassium channels and TRPs are also expressed in a cell specific manner, displaying

a scattered distribution within populations (Fig. S13). Thus, the communication of mature oligodendrocytes with neighbouring neurons might be mediated through specific receptors and channels, following synaptic input or vesicular release.

Our study provides a high-resolution view of the transcriptional landscape of a single neural subtype across multiple regions of the CNS, and indicates a transcriptional continuum between oligodendrocyte populations, with a subset of them representing distinct but nevertheless connected stages in the maturation path from an OPC to mature oligodendrocytes (Fig. S15). We find that this path for differentiation is ubiquitous throughout the CNS, suggesting that mature oligodendrocyte subtype specification occurs later at postnatal stages in a region specific manner (Fig. S15). Future investigations will determine whether this is unique to the oligodendrocyte lineage or whether neuronal populations can also be specified later in development and not only at neural progenitor stage (*32*). We identify six distinct populations of mature oligodendrocytes, which are present predominantly in specific CNS regions (Fig. S15). As such, each brain region appears to optimize its circuitry by representation of unique proportions and combinations of mature oligodendrocytes.

The traditional view of oligodendrocytes as merely myelin sheath forming cells whose main function is to increase the speed of action potentials, is starting to evolve into a more complex picture. The transcriptional profile of mature oligodendrocytes suggests heterogeneity as well as previously unidentified functions in the neural circuitry in the CNS. Our data also indicate that Itpr2+ oligodendrocytes are involved in rapid myelination in complex motor learning and thus might be relevant in other active maturation/myelination processes in the adult, such as myelin remodeling or remyelination in disease/lesion paradigms. Non-proliferative Nkx2.2+ precursors with a profile consistent with these cells (Fig. S9) have been observed in lesions of multiple sclerosis patients (*33*). Therefore our study, by establishing oligodendrocytes as a transcriptionally heterogeneous cell lineage, might lead to new insights into the aetiology of myelin disorders such as multiple sclerosis.and suggest novel targets for their treatment.

Figure 1 – Single cell RNA-Seq reveals 13 populations of cells with markers of the oligodendrocyte lineage in ten regions of the mouse CNS.

(A) Dissection scheme for the ten CNS regions analysed by single cell RNA-Seq. (B) Number of cells analysed for each region. (C) Dendrogram of oligodendrocyte populations as reconstructed by linkage clustering (left panel). Heatmap described the correlation between each pair of clusters (middle panel). Abundance of each of the subclasses along the different CNS regions is represented by the area of the circles (right panel).

Figure 2 – Intermediate oligodendrocyte cell states in the continuous maturation process from precursors to mature cells.

(A) tSNE projection of 5072 cells analysed showing transition from OPCs to mature oligodendrocytes. Pdgfra+ vascular and leptomeningeal cells (VLMCs) were distinct. (B) Average (±s.e.m.) expression for marker genes for OPCs, differentiated-committed precursors and VLMCs populations. The expression of representative markers is overlayed on the tSNE map. gray = low expression and red = high expression. (C) The expression of cell-cycle genes is overlayed on the tSNE projection showing localization of cycling cells within the OPC population. Table describe statistical enrichment (hypergeometric test) of cell-cycle genes to the

OPC compared to the overall population. (D-E) smFISH validation of distinct cell identities. (D) smFISH confirms that committed oligodendrocyte precursors expressing *Neu4* are also positive for *Itpr2* and *Sox10;* (E) smFISH for *Sox10, Ctps* (myelin-forming oligodendrocytes marker) and *Klk6* (mature oligodendrocytes marker) confirm these populations are distinct. (F) Pseudo-time analysis along the path along the center of the cloud, representing trajectory from OPC to myelin forming oligodendrocytes. Heatmap shows smoothed pseudo-time dependent genes with representative examples for early, intermediate and late genes. (G) Immunohistochemistry of Col1a1 (VLMCs marker), Pdgfra (OPC and VLMCs marker) and Tomato lectin (marker of blood vessels) in P21 brain, shows that the VLMCs are exclusively in the vessels (white arrowhead) while OPCs (Col1a1-) are in the parenchyma and following blood vessels trails – yellow arrowhead. Scale bar 25μm.

Figure 3 – Itpr2+ oligodendrocytes are derived from OPCs, are present in regions of active differentiation and increase in mice undergoing learning in the complex wheel paradigm

(A) Average (±s.e.m.) expression level of *Tcf7l2*, *Itpr2*, *Tmem2* and *Pdgfa* along the oligodendrocyte lineage. The expression of each marker is overlayed on the tSNE map (right). (B) No colocalization of Itpr2+ cells (red) with Pdgfra+ cells (green) by immunohistochemistry in P21 brain. (C) In hippocampus, corpus callosum and cortex, Itpr2+ (red) were co-localized with GFP+ cells in P21 *Pdgfra*-H2B-GFP mice. Quantification of Itpr2+/GFP+ cells in the three brain regions. One-way ANOVA with Tukey´s multiple comparison test. **p<0.01; ***p<0.001. n=3 (D, E) Immunohistochemistry and quantification of % Itpr2+/Sox10+ in P7, P21 and P90 brain. One-way ANOVA with Tukey´s multiple comparison test *p<0.05, n=3. (F) Immunohistochemistry of Sox10 and Itpr2 in non-runners versus runners P60 brain after 2 days in the complex wheel-learning paradigm. (G) Quantification of % Itpr2+/Sox10+ in corpus callosum showed an increase of ~50% in committed precursors/newly formed oligodendrocytes density when learning to run on the complex wheel for 2 days (p-value represents one-tail t-test). Scale bars – 75 μm.

Figure 4 – Region and age specific distribution of mature oligodendrocytes

(A) tSNE projections (as Fig2A); in each panel colored dots represent cells from one of the ten CNS regions analyzed, whereas gray dots represent the remaining cells in the dataset. Brain regions were separated into immature, intermediate and mature, according to the abundance of different stages in the maturation process. (B) Age comparison of observed OL population in cortex S1 (left) or corpus callosum (right). Cells from juvenile (red) or adult (blue) mice are overlaid on the tSNE projection. Bar-plots show the percentage of each population in age group (bottom panel).

References

1. N. Kessaris *et al.*, Competing waves of oligodendrocytes in the forebrain and postnatal elimination of an embryonic lineage. *Nat Neurosci* **9**, 173-179 (2006).
2. P. d. Rio-Hortega, Tercera aportacion al conocimiento morfologico e interpretacion funcional de la oligodendroglia. *Mem Real Soc Espan Hist Nat* **14**, 40 –122 (1928).
3. G. S. Tomassy *et al.*, Distinct profiles of myelin distribution along single axons of pyramidal neurons in the neocortex. *Science* **344**, 319-324 (2014).
4. R. B. Tripathi *et al.*, Dorsally and ventrally derived oligodendrocytes have similar electrical properties but myelinate preferred tracts. *J Neurosci* **31**, 6809-6819 (2011).

5.   M. E. Bechler, L. Byrne, C. Ffrench-Constant, CNS Myelin Sheath Lengths Are an Intrinsic Property of Oligodendrocytes. *Curr Biol* **25**, 2411-2416 (2015).

6.   A. Zeisel *et al.*, Brain structure. Cell types in the mouse cortex and hippocampus revealed by single-cell RNA-seq. *Science* **347**, 1138-1142 (2015).

7.   H. Kettenmann, H. Kettenmann, B. R. Ransom, *Neuroglia*. (Oxford University Press, Oxford ; New York, ed. 3rd, 2013), pp. xxii, 930 p.

8.   K. M. Young *et al.*, Oligodendrocyte dynamics in the healthy adult CNS: evidence for myelin remodeling. *Neuron* **77**, 873-885 (2013).

9.   L. Dimou, M. Gotz, Glial cells as progenitors and stem cells: new roles in the healthy and diseased brain. *Physiol Rev* **94**, 709-737 (2014).

10.   C. C. Stolt *et al.*, SoxD proteins influence multiple stages of oligodendrocyte development and modulate SoxE protein function. *Dev Cell* **11**, 697-709 (2006).

11.   J. Samanta, J. A. Kessler, Interactions between ID and OLIG proteins mediate the inhibitory effects of BMP4 on oligodendroglial differentiation. *Development* **131**, 4131-4142 (2004).

12.   Y. Chen *et al.*, The oligodendrocyte-specific G protein-coupled receptor GPR17 is a cell-intrinsic timer of myelination. *Nat Neurosci* **12**, 1398-1406 (2009).

13.   J. D. Cahoy *et al.*, A transcriptome database for astrocytes, neurons, and oligodendrocytes: a new resource for understanding brain development and function. *J Neurosci* **28**, 264-278 (2008).

14.   V. A. Swiss *et al.*, Identification of a gene regulatory network necessary for the initiation of oligodendrocyte differentiation. *PLoS One* **6**, e18088 (2011).

15.   Y. Zhang *et al.*, An RNA-sequencing transcriptome and splicing database of glia, neurons, and vascular cells of the cerebral cortex. *J Neurosci* **34**, 11929-11947 (2014).

16.   F. Ye *et al.*, HDAC1 and HDAC2 regulate oligodendrocyte differentiation by disrupting the beta-catenin-TCF interaction. *Nat Neurosci* **12**, 829-838 (2009).

17.   E. Chow *et al.*, Disrupted compaction of CNS myelin in an OSP/Claudin-11 and PLP/DM20 double knockout mouse. *Mol Cell Neurosci* **29**, 405-413 (2005).

18.   C. Trapnell *et al.*, The dynamics and regulators of cell fate decisions are revealed by pseudotemporal ordering of single cells. *Nature biotechnology* **32**, 381-386 (2014).

19.   R. A. Klinghoffer, T. G. Hamilton, R. Hoch, P. Soriano, An allelic series at the PDGFalphaR locus indicates unequal contributions of distinct signaling pathways during development. *Dev Cell* **2**, 103-113 (2002).

20.   K. Roesch *et al.*, The transcriptome of retinal Muller glial cells. *J Comp Neurol* **509**, 225-238 (2008).

21.   H. H. Tsai *et al.*, Oligodendrocyte precursors migrate along vasculature in the developing nervous system. *Science* **351**, 379-384 (2016).

22.   J. Levine, The reactions and role of NG2 glia in spinal cord injury. *Brain Res*, (2015).

23.   H. Fu, S. Kesari, J. Cai, Tcf7l2 is tightly controlled during myelin formation. *Cell Mol Neurobiol* **32**, 345-352 (2012).

24.   K. Hamano *et al.*, A quantitative study of the progress of myelination in the rat central nervous system, using the immunohistochemical method for proteolipid protein. *Brain Res Dev Brain Res* **108**, 287-293 (1998).

25.   I. A. McKenzie *et al.*, Motor skill learning requires active central myelination. *Science* **346**, 318-322 (2014).

26.   J. M. Levine, R. Reynolds, J. W. Fawcett, The oligodendrocyte precursor cell in health and disease. *Trends Neurosci* **24**, 39-47 (2001).

27.   H. C. Kinney, B. A. Brody, A. S. Kloman, F. H. Gilles, Sequence of central nervous system myelination in human infancy. II. Patterns of myelination in autopsied infants. *J Neuropathol Exp Neurol* **47**, 217-234 (1988).

28.   B. A. Brody, H. C. Kinney, A. S. Kloman, F. H. Gilles, Sequence of central nervous system myelination in human infancy. I. An autopsy study of myelination. *J Neuropathol Exp Neurol* **46**, 283-301 (1987).

29.   J. C. Coffey, K. W. McDermott, The regional distribution of myelin oligodendrocyte glycoprotein (MOG) in the developing rat CNS: an in vivo immunohistochemical study. *J Neurocytol* **26**, 149-161 (1997).

30.   I. Micu *et al.*, The molecular physiology of the axo-myelinic synapse. *Exp Neurol* **276**, 41-50 (2016).

31.   N. B. Hamilton, K. Kolodziejczyk, E. Kougioumtzidou, D. Attwell, Proton-gated Ca(2+)-permeable TRP channels damage myelin in conditions mimicking ischaemia. *Nature* **529**, 523-527 (2016).

32.   L. Telley *et al.*, Sequential transcriptional waves direct the differentiation of newborn neurons in the mouse neocortex. *Science*, (2016).

33.   T. Kuhlmann *et al.*, Differentiation block of oligodendroglial progenitor cells as a cause for remyelination failure in chronic multiple sclerosis. *Brain* **131**, 1749-1758 (2008).

Any Additional Author notes:

SM, AZ, HL, WDR, SL and GC-B designed the experiments. PE, EA, JH-L, TB, WDR, SL and GC-B, senior authors, obtained funding. SM, AZ, SC, HH, RAR, DG, MH, AMM, GLM, FR, HL, LX, EF performed the experiments. LX, HL and WDR have priority of observation of the rapid differentiation of oligodendrocytes in the complex motor wheel paradigm. SM, AZ, DvB, AMF, GLM, PL analysed data. SM, AZ, SL and GC-B wrote the paper, with the assistance and proofreading of all authors.
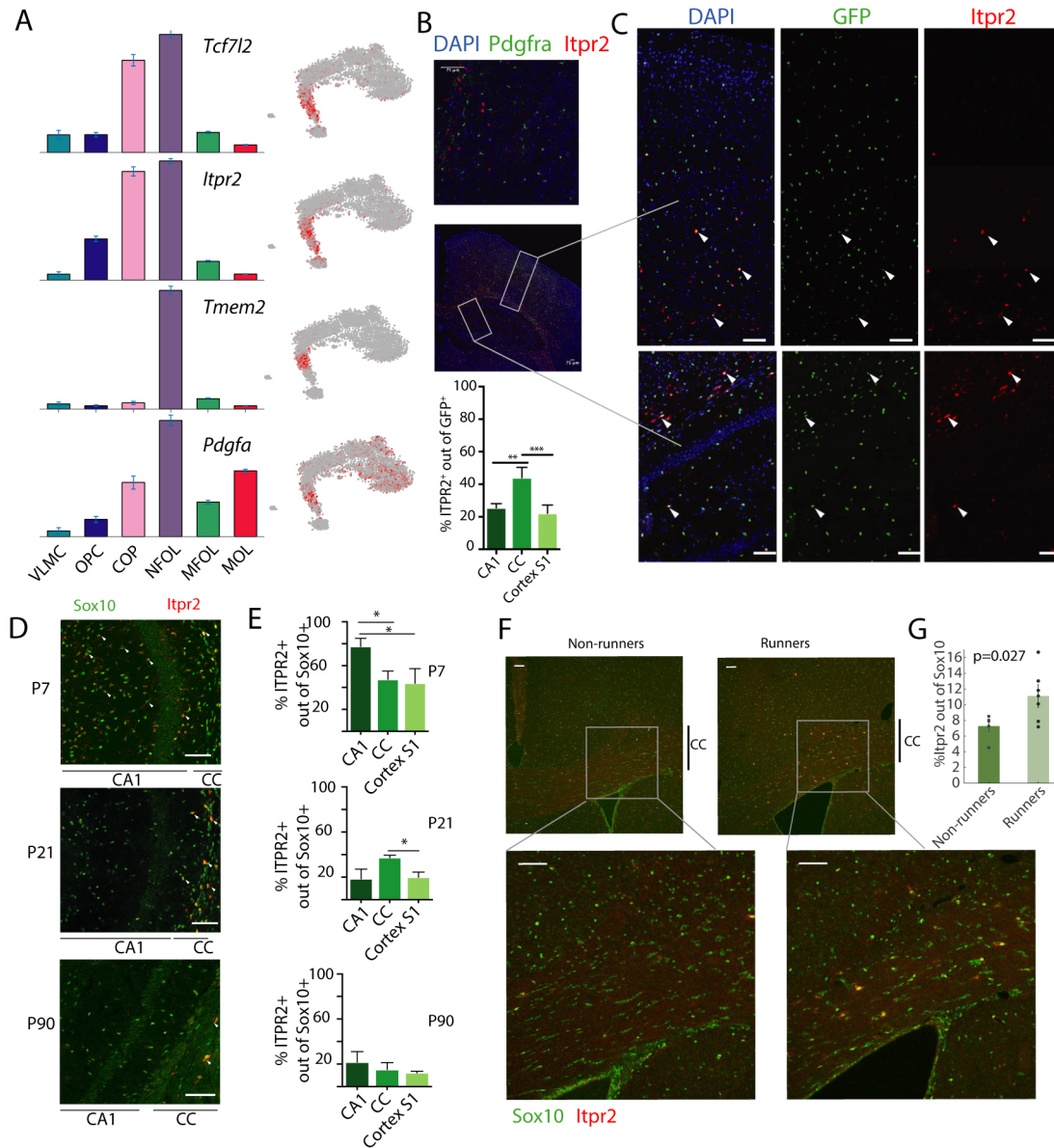
Marques and Zeisel et al, Figure 1:
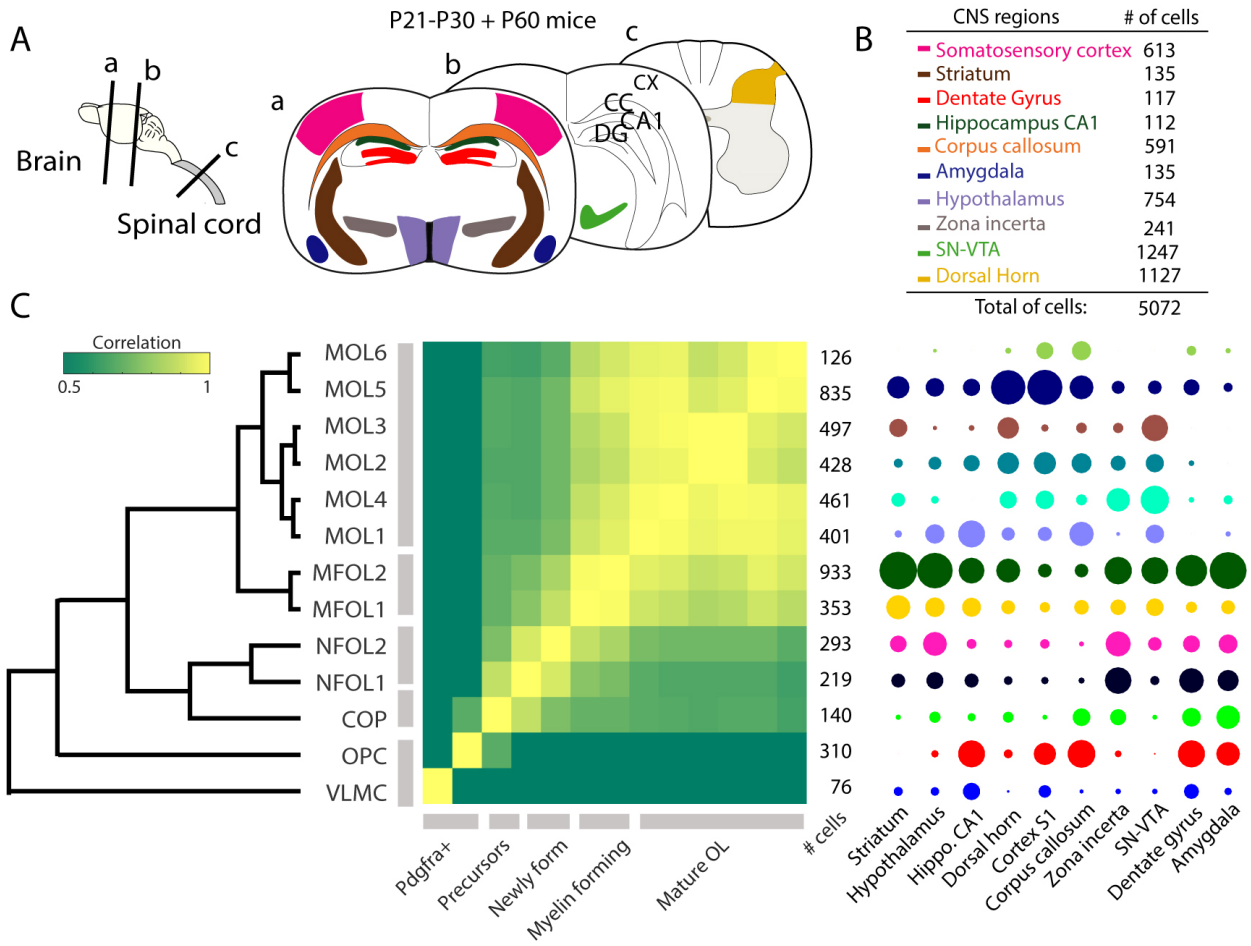
Marques and Zeisel et al, Figure 2
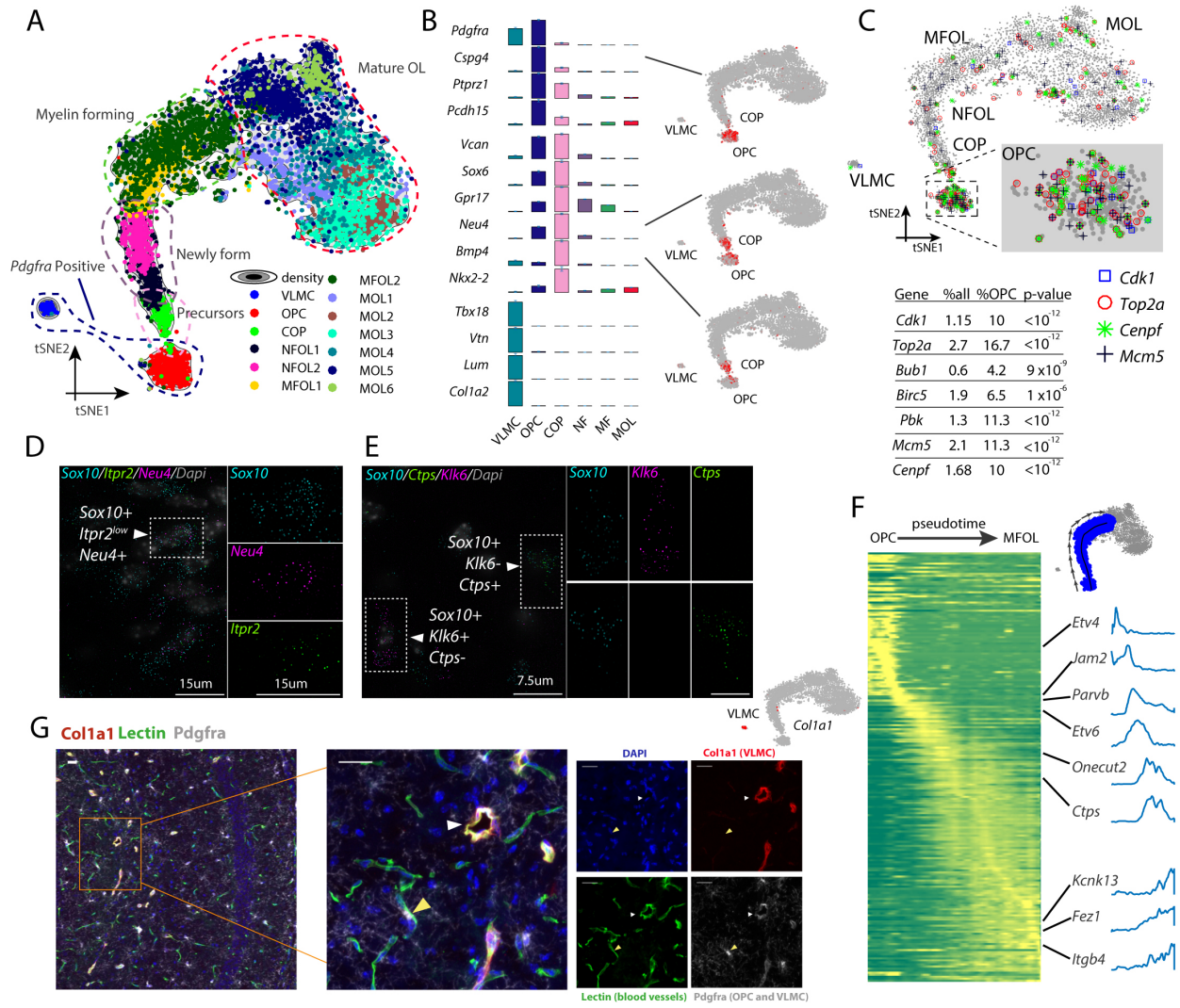
Marques and Zeisel et al, Figure 3:

Marques and Zeisel et al, Figure 4: